Speciation and ammonia-induced precipitation of neptunium and uranium ions

Gregory Leinders,[a,*] Beatriz Acevedo,[a] Frédéric Jutier,[a] Gamze Colak,[a,b] Marc Verwerft [a]

[a] Belgian Nuclear Research Centre (SCK CEN), Institute for Nuclear Materials Science, Boeretang 200, B-2400 Mol, Belgium.

[b] KU Leuven, Department of Materials Engineering, Kasteelpark Arenberg 44, B-3001 Leuven, Belgium

Abstract

The pH evolution and corresponding changes in the UV-Vis-NIR absorption spectra of oxygenated neptunium (NpO_2^+ and NpO_2^{2+}) and uranyl ions (UO_2^{2+}) in nitric acid are investigated during titration with aqueous NH_3 solution. The speciation and precipitation regimes between acidic (pH 1.5) and alkaline (pH 10) conditions at room temperature are discussed to assess the suitability of Np(V) or Np(VI) in sol-gel conversion processes for fuel target fabrication. Under the applied experimental conditions, Np(V) hydrolyzes and precipitates into the insoluble hydroxide NpO_2OH only above pH values 7.5 and an increase up to pH 10.0 is required to precipitate quantitatively. Np(VI) displays changes in the coordination environment of NpO_2^{2+} ions in the pH interval 1.6 to 4.0, similar to what is observed for U(VI). Precipitation into $NpO_3{\cdot}H_2O$ or other hydroxide compounds takes place between pH 4.0 – 5.9, which overlaps largely with precipitation of ammonium diuranate species from U(VI) solution. The use of concentrated NH_3 aqueous solution, as commonly used in the external gelation process, allows to quantitatively precipitate both Np(V) and Np(VI) species. Internal gelation process conditions, on the other hand, seem incompatible with the high pH required to precipitate Np(V) completely. For fabricating mixed-oxide (U,Np) targets using sol-gel conversion, a feed broth containing Np(VI) and U(VI) will be required to achieve homogenous gelation.

[*] Corresponding author
E-mail address: gregory.leinders@sckcen.be (G. Leinders)
Phone: +32 14 33 31 63

1. Introduction

Neptunium-237 (^{237}Np) is one of the so-called Minor Actinide (MA) elements which are formed during irradiation of nuclear fuel in a nuclear reactor. Together with certain isotopes of plutonium and americium, it dominates the long term radiotoxicity of spent Light Water Reactors (LWR) fuel [1]. In principle, Np can be partitioned from the spent nuclear fuel in the industrially applied processes for uranium and plutonium recovery.[1,2] The partitioning of long-lived MAs such as ^{237}Np from the spent nuclear fuel and their transmutation in fast neutron spectrum reactors have been identified as a possible strategy to reduce the long-term impact of spent nuclear fuel, as compared to a direct disposal scenario.[3] Depending on the specific strategy, the transmutation targets can consist of fissile or inert matrices (e.g. UO_2, $(U,Pu)O_2$, ZrO_2, MgO, Mo) which contain the MA element in solid solution or in a composite form.[4] In a completely different domain, ^{237}Np is the parent isotope for the production of plutonium-238 (^{238}Pu), which is the preferred isotope for radioisotope thermoelectric generators (RTG), used since the earliest days of space exploration and still in use for today's spatial missions far from the Sun. ^{238}Pu has a high-power density, an almost total absence of penetrating gamma radiation and a relatively long half-life of 87.7 years.[1,5,6] Production of ^{238}Pu proceeds via neutron irradiation of $^{237}NpO_2$-bearing targets.[1,5-7]

The fabrication of $^{237}NpO_2$-bearing targets is confronted with radiological risks due to the nature of the ^{237}Np nuclide which is an alpha emitter ($T_{1/2} = 2.14 \times 10^6$ years), and in particular also due to its ^{233}Pa daughter. At secular equilibrium, one gram of ^{237}Np contains 25.9×10^6 Bq of ^{233}Pa ($T_{1/2} = 27$ days), decaying through beta-decay and emitting an energetic gamma ray (0.31 MeV).[2] For handling trace amounts of Np, the gamma radiation dose is manageable, but this is no longer the case when larger scale productions are aimed at. Hence, target fabrication routes making use of aqueous conversion processes are being investigated to minimize radiological hazards related to the handling of Np-containing materials.[8-10] In particular, the use of sol-gel techniques, in which liquid "sol" droplets are directly converted into solid or "gelled" kernels, are of interest because the obtained spherical kernels have many advantages with respect to handling and processing into targets.[11-13] The two main processes used for conversion of actinide nitrate solutions into microspheres are the external gelation process in which solution droplets are converted to gelled particles by contact with gaseous and/or liquid ammonia aqueous solution, and the internal gelation process in which hydrolysis of the metal ions takes place by the *in-situ* generation of ammonia during thermal decomposition of the gelation agents hexamethylenetetramine and urea.[13-16]

Sol-gel processes allow to produce actinide oxide microspheres *e.g.* UO_2, PuO_2 and ThO_2, as well as mixed-oxide or composite microspheres, such as $(U,Th)O_2$, $(U,Pu)O_2$, and MA-bearing microspheres.[17-23] The approach to fabricate such mixed-oxides is to mix the uranium feed broth with a solution containing the dopant, and to process this "*metal blend*" solution in the same manner as the conventional feed broth.[12,24-26] The hydrolysis behaviour of the individual metal ions during the gelation reaction affects the quality of the microspheres. An inhomogeneous mixing of the dopant element into the uranium matrix occurs if the precipitation pH of the individual ions diverge significantly, as is *e.g.* the case for Ce^{4+} and UO_2^{2+} ions,[27] and premature or incomplete gelation can take place. Hence, prior to fabricating oxide microspheres using gelation processes, a feasibility study is required to investigate the hydrolysis behaviour of the metal ions and to evaluate how it may affect the overall gelation reaction.

In acidic aqueous conditions with high ionic strength neptunium may assume oxidation states varying from Np(III) to Np(VI),[28-32] although Np(III) is generally not present in oxidizing acidic media.[28] The Np(III) and (IV) states exist as hydrated cations (Np^{3+} and Np^{4+}) in acidic solutions, the tetravalent Np ion being coordinated by hydrated water molecules or bidentate-coordinating nitrate ions (depending on the nitrate concentration).[33] Np ions with the higher oxidation states behave as strong Lewis acids and exist as oxygenated ions such as NpO_2^+ and NpO_2^{2+}.[29,30] Both type of ions are coordinated by hydrated water molecules, or in combination with bidentate-coordinating nitrate ions, in the equatorial plane.[33]

The Np(V) compound, NpO_2^+, is the most stable state of Np ions in acidic solution unless an oxidizing or reducing agent is present to adjust the oxidation state[28,34-36] The speciation in nitric acid is peculiar,[36,37] and under high acidic concentrations (e.g. 5 to 9 M nitric acid) the NpO_2^+ ion can disproportionate to Np^{4+} and NpO_2^{2+} resulting in a mixed-valence Np solution.[28,29] While oxidation of NpO_2^+ to the hexavalent state NpO_2^{2+} takes place *via* a simple electronic exchange, reduction to Np^{4+} involves the breaking of Np-O bonds, making this step generally slower.[38] Under alkaline conditions Np(V) is hydrolyzed, but the speciation is sensitive to the background electrolyte,[39] and to the presence of carbonate ions.[29,40,41] In carbonate-free $NaClO_4$ solution (0.1 M) no significant hydrolysis of NpO_2^+ takes place at pH below 10.[40] At higher pH, with a maximum around pH 11.5, the insoluble hydroxide NpO_2OH (grey-white precipitate) is formed, while at a pH above 12 the hydroxo complex $NpO_2(OH)_2^-$ becomes predominant. Several studies reported on the susceptibility to CO_2

absorption, which causes carbonate complexation, significantly affecting the hydrolytic behavior,[29,41-44] and on shifts in equilibria as function of temperature.[41,45]

The Np(VI) ion NpO_2^{2+} is less stable than the hexavalent UO_2^{2+} and PuO_2^{2+} ions and is hydrolyzed quickly into polynuclear hydroxo complexes such as $(NpO_2)_2(OH)_2^{2+}$.[29,46,47] An exchange between hydrated water molecules and nitrate ions can take place, depending on the nitrate concentration.[33] Similar as with Np(V), carbonate complexation may occur, and hydrolysis experiments on Np(VI) in a $NaClO_4$ solution (0.1 M) at either 80% or 0.03% CO_2 partial pressure resulted in precipitation of NpO_2CO_3 (tan greenish powder), or $NpO_3{\cdot}H_2O$ (dark reddish brown powder), respectively, rather than the hydroxide $NpO_2(OH)_2$.[48]

Within this work, the speciation of oxygenated neptunium ions (NpO_2^+ and NpO_2^{2+}) and of uranyl ions (UO_2^{2+}) in aqueous solution were investigated. Specifically, the evolution and precipitation regimes during titration with ammonia between acidic (pH 1.5) and alkaline (pH 10) conditions, relevant for sol-gel processes, were assessed. The aim was to evaluate conditions for the production of NpO_2 or mixed uranium-neptunium oxide microspheres by applying internal or external gelation processes.

2. Materials and methods

2.1.Chemicals

Depleted uranium dioxide powder (UO_2, 0.32 wt.% ^{235}U, nuclear grade impurity level) originated from a stock originally supplied by AREVA (France). Neptunium dioxide powder ($^{237}NpO_2$, isotopically pure) was obtained from JRC Geel (Belgium). Nitric acid aqueous solution ($w(HNO_3)$ = 68 wt.%, purity > 99.9 wt.%) and ammonia aqueous solution ($w(NH_3)$ = 30 wt.%, purity > 99.5 wt.%) were purchased from Sigma-Aldrich. Sodium nitrite ($NaNO_2$, purity > 99.0 wt.%) was purchased from VWR. Sodium hydroxide pellets (NaOH, purity 99 wt.%) were purchased from Thermo Fisher Scientific.

2.2.Preparation of neptunium and uranium stock solutions

Neptunium dioxide powder (370 mg) was first calcined in 250 ml·min^{-1} of air up to 700 °C for 12 h in a LOBA GLB 1200 tube furnace (HTM Reetz GmbH) located in a glove-box. The purpose was to ensure that the neptunium dioxide is in a pure and stoichiometric form since it might have reduced slightly to NpO_{2-x} after storage, as reported in literature.[49] The calcined NpO_2 powder was subsequently dispersed with a known amount of Milli-Q water in a closed recipient and transferred from glove-box to fume hood environment where a dissolution in nitric acid under reflux conditions was performed. The reflux setup consisted of a 25 ml three neck round-bottom flask with a stirring magnet, placed in a DrySyn block on a heating/stirring plate with thermocouple control (VWR advanced VMS-C7). The middle neck was fitted with a double-walled condenser, connected to a recirculating cooling bath (Buchi F-105) set to 9 °C to restrict the evaporation from the flask during refluxing. To capture any remaining vapors, the top of the condenser was connected to a vacuum pump (Buchi V-700) with the gas passing through two washing bottles containing a NaOH solution (1 mol L^{-1}). One side neck was closed off using a glass stopper. The other side neck was used to add reagents or sample volumes using an Eppendorf Research Plus volumetric pipet. During the intermittent times, the neck was closed off using a glass stopper.

The NpO_2 dispersion in Milli-Q water was poured into the round-bottom flask. The recipient was rinsed twice with Milli-Q water and twice with HNO_3 (aq., 4 mol L^{-1}), each amount measured to take into account in the mass balance. The HNO_3 concentration in the flask at the start of the reflux treatment was 0.66 mol L^{-1}. The procedure was carried out over multiple days, owing to the relatively slow dissolution kinetics under the applied conditions. Despite the application of reflux conditions a reduction in solution volume over the course of the

experiment was observed, caused by incomplete condensation of evaporated gasses. To compensate for the volume reduction and to further promote the dissolution reaction, a small supplement of aqueous nitric acid solution (4 mol L^{-1}) was added to the flask after 15 h of refluxing. After 4 more hours of refluxing an aliquot of approximately 2.6 mL Np solution was recovered. The solution was first passed over a Whatman cat. 1450-090 paper filter (particle retention: 2.7 µm) in order to remove remaining undissolved powder or otherwise undissolved residues. The round-bottom flask was rinsed with a known amount of Milli-Q water, the rinsing water being used to wash the filter and collected together with the filtrate to obtain a stock solution with a Np concentration of 15.7 ± 1.6 mg/g (determined quantitatively by by inductive coupled plasma mass spectrometry (Thermo Scientific Element 2 HR-ICP-MS, calibrated with external Np-237 standard solutions). The density of the stock solution was measured to be 1.027 ± 0.005 g/mL, from which the molar concentration of $c(Np)_{stock}$ = 0.068 ± 0.007 mol L^{-1} was calculated. A detailed qualification of this solution using UV-Vis-NIR spectrophotometry is reported further down in section 3.1.

UO_2 powder was first converted into U_3O_8 by calcination at 550 °C (2 h isotherm) under atmospheric air in a muffle furnace (Nabertherm LT 9/13/P330). Uranyl nitrate (UN) aqueous solution was subsequently prepared by dissolving U_3O_8 in stoichiometric amounts of HNO_3 (aq., 4.45 mol L^{-1}). Dissolution was first performed at room temperature, during continuous stirring until a yellow-colored solution was observed. To ensure the complete dissolution of any remaining U_3O_8, the solution was briefly heated to 70 °C while maintaining stirring until a transparent yellow solution was obtained. After cooling down to room temperature the pH (0.47) and density (1.777 g/mL) were measured. Lastly, the uranium concentration of the UN solution (2.37 mol L^{-1}) was measured precisely by ICPMS (Thermo Scientific Element 2 HR-ICP-MS, calibrated with certified U stock solutions. The UV-Vis-NIR spectrum of a diluted aliquot showed the typical signature of uranyl (UO_2^{2+} ions) in solution, see Figure S1 in the ESI.

2.3.Hydrolysis experiments

Room-temperature hydrolysis experiments were carried out on solutions diluted from each stock solution (c(U), c(Np) = 0.01 mol L^{-1}). During an experiment, a titration with NH_3 aq. solution was carried out such that 0.1 mol NH_3 per mol uranium or neptunium was added at a 1 minute time interval, while stirring the solution. The ionic strength of the solution was therefore continuously changing, having values of the order 0.1 mol L^{-1}. The setup consisted of a three neck round-bottom flask with a stirring magnet, equipped with a pH-temperature

electrode in one side neck. The middle neck was closed with a glass stopper, while the remaining neck was used to add reagents or sample volumes using an Eppendorf Research Plus volumetric pipet. The pH evolution was measured continuously at a 5 sec interval during the whole duration of the experiment (ca. 90 minutes). Small aliquots (180-380 µL) were sampled from the solution at a 2 minute interval and stored in closed vials for subsequent analysis using UV-Vis-NIR spectrophotometry. All aliquots were left to settle for 3-4 hours, in order to allow transferring only the supernatant solution into the cuvettes whenever precipitates were present.

2.4.pH Measurements

The pH of the samples was measured using a ScienceLine plus pH "micro" combination electrode (SI Analytics), designed for measuring low volume samples. It employs a Silamid® double junction reference system (Ag/AgCl) ensuring fast and stable measurements, with an outer bridge electrolyte solution of KCl (3 mol L^{-1}). Data acquisitions were digitally logged using a WTW ProfiLine pH 3310 meter at a 5 sec interval during the course of the experiments. The raw pH data were smoothed using adjacent-averaging with a window size of ten data points in OriginLab 2023 to allow further processing. A four-point calibration of the pH electrode was always performed just before launching the data acquisition. For this purpose we used WTW standard buffer solutions PL 2 and PL 4 (pH 1.68 and 4.01 ± 0.02 at 25 °C, respectively), and WTW technical buffer solutions TPL 7 and TPL 10 Trace (pH 7.00 and 10.01 ± 0.03 at 25 °C, respectively), traceably certified to PTB and NIST. Excellent linearity in the pH response was obtained, with slope and zero point values well within specifications: between -59.8 to -57.4 mV pH^{-1} and between pH 6.75 to 7.25, respectively. The propagated uncertainty was evaluated at ±0.05 pH units (2σ). No ionic strength adjustment factor was applied considering the fairly low ionic strength of the solutions (of the order 0.1 mol L^{-1}).All measurements were performed at room temperature and during stirring of the solution.

2.5.UV-Vis-NIR spectrophotometry

A Shimadzu UV2600 outfitted with the ISR-2600Plus two-detector integrating sphere was used to measure absorption spectra over the range 220 to 1400 nm, *i.e.* from the ultra-violet (UV) over to the visible (Vis) spectrum, up to the near-infrared (NIR) region. The photometric and wavelength accuracy were validated using a set of glass filters, and the spectral resolution was verified using a filter set containing toluene in hexane (purchased from Hellma). Quartz glass high performance cuvettes with a nominal volume of 160 µL and an

optical path length of 10 mm were used (Hellma 105-200-15-40). A polyethylene stopper on the cuvettes ensured a safe transfer of the filled cuvettes from the working environment in the fume hood to the sample loading station of the spectrophotometer. Data acquisition was performed with the software package *UVProbe* by Shimadzu (Version 2.62). Conversion of the output files into text-based files for further processing was done using SpectraGryph 1.2.[50]

Measurements on neptunium solutions were performed between 220 and 300 nm using the D2 (deutrerium) lamp, and between 300 and 1300 nm using the WI (halogen) lamp. Absorbance in the UV to VIS spectrum (up to 860 nm) was acquired using the photomultiplier detector, the nIR spectrum was measured using the InGaAs detector. A step size of 1.0 nm and acquisition time of 0.2 sec was used. The slit width was set to 2.0 nm. Measurements on uranium solutions were performed between 310 and 550 nm, using the WI (halogen) lamp. A step size of 0.5 nm and acquisition time of 1 sec was used. The slit width was set to 2.0 nm. All spectra reported from the hydrolysis experiments were corrected for the effect of dilution due to titration with NH_3 aq. solution and the removal of solution volume for UV-Vis-NIR analysis, by multiplication of a scale factor based on the measured amounts. Milli-Q water was used to measure the baseline of all reported spectra.

3. Results

3.1.Qualification of the Np stock solution

The absorption spectra of neptunium in aqueous solutions have been used in several studies [40,41,45,51-54] to provide straightforward identification of the Np speciation, Np dissolution or hydrolysis reactions with different experimental conditions. Each oxidation state shows characteristic absorption bands sufficiently differentiated from each other, which allow a spectrophotometric analysis of the mixtures. The absorption spectrum of the Np stock solution prepared for this work is presented in Figure 1. A comparison is made against reference spectra of Np(V) and Np(VI) in matching aqueous conditions reported in literature.[45] The solution clearly consists of a Np(V)-Np(VI) mixture, without detectable amounts of Np(III) or Np(IV).

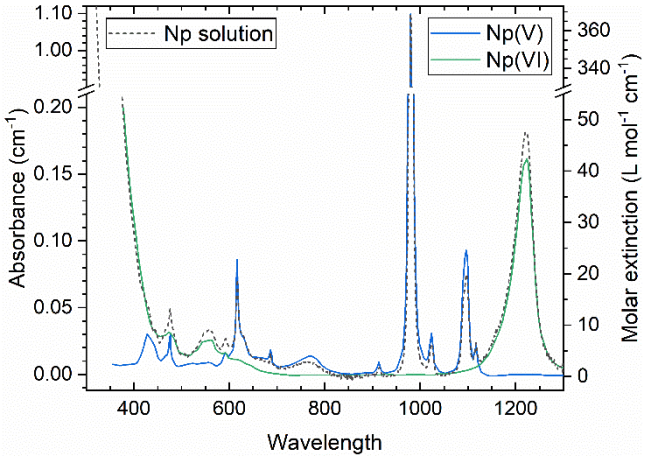

Figure 1. (black, dashed line) Absorption spectrum of the Np stock solution prepared in this work, diluted in a 1:10 volumetric ratio with Milli-Q water to c(Np) = 6.8 mmol L^{-1}. (colored, solid lines) Reference spectra of single-valence Np(V) and Np(VI) solutions in nitric acid ($c(HNO_3)$ = 0.5 mol L^{-1}), reproduced from graphical data reported by Friedman and Toth using the Engauge Digitizer Software developed by Mark Mitchell *et al.*[45,55] These data are expressed in molar extinction units (L mol^{-1} cm^{-1}) on the right-hand side abscissa.

The Np aqueous system follows the Beer-Lambert law, and hence, the measured absorbance at a given wavelength (A_λ) is related to the concentration of Np ions (c(Np(V) and c(Np(VI) in the present case), and their respective molar extinction coefficients (ε_λ).[56] Therefore, by choosing two absorption bands, a system of two equations is obtained from which the individual fractions of Np(V) and Np(VI) can be derived:

$$A_\lambda = \varepsilon_\lambda^{\mathrm{Np(V)}} \times c\big(\mathrm{Np(V)}\big) + \varepsilon_\lambda^{\mathrm{Np(VI)}} \times c\big(\mathrm{Np(VI)}\big) \quad \text{(Eq. 1)}$$

$$\begin{cases} A_{1097} = \varepsilon_{1097}^{\mathrm{Np(V)}} \times c\big(\mathrm{Np(V)}\big) + \varepsilon_{1097}^{\mathrm{Np(VI)}} \times c\big(\mathrm{Np(VI)}\big) \\ A_{1223} = \varepsilon_{1223}^{\mathrm{Np(V)}} \times c\big(\mathrm{Np(V)}\big) + \varepsilon_{1223}^{\mathrm{Np(VI)}} \times c\big(\mathrm{Np(VI)}\big) \end{cases} \quad \text{(Eq. 2)}$$

In this work, the two distinct absorption bands in the near-infrared region with local maxima at 1097 nm and at 1223 nm, which are associated predominantly to Np(V) and Np(VI), respectively, will be used. Note that the strong absorption band associated to the free NpO_2^+ ion, occurring at 980 nm,[41] was not selected for this purpose to avoid a bias when approaching detector saturation. The corresponding molar extinction coefficients are deduced from Figure 1 and reported in **Table 1**. Based on the measured absorbance and by applying (Eq. 2) the corresponding Np concentrations are solved as 0.028 mol L^{-1} Np(V) and 0.042 mol L^{-1} Np(VI). We note that this ratio of Np(V) to Np(VI) ions was not fixed *a priori*, but it resulted from the chosen dissolution conditions (see §2.2). Consequently, the nominal Np concentration is equal to 0.070 mol L^{-1}, which is in excellent agreement with the total Np concentration measured by ICPMS (0.068 ± 0.007 mol L^{-1}). This verifies the approach to estimate Np concentrations based on reported molar extinction coefficients in similar aqueous conditions.

Table 1. Molar extinction coefficients for Np(V) and Np(VI) solutions in 0.5 mol L^{-1} HNO_3 at specified wavelengths. Values were estimated from graphical data reported by Friedman and Toth.[45]

	Np(V)	**Np(VI)**
λ (nm)	**ε_λ (L mol^{-1} cm^{-1})**	**ε_λ (L mol^{-1} cm^{-1})**
1097	24.7	1.2
1223	0.5	43.1

3.2.Hydrolysis in a mixed Np(V)/Np(VI) solution

The pH evolution in the mixed Np(V)/Np(VI) stock solution as function of added NH_3 aq. solution (expressed as the molar ratio of NH_3 (aq.) to initial neptunium during the experiment, $n(\mathrm{NH_3}) \cdot n(\mathrm{Np})_{\mathrm{initial}}^{-1}$) is presented in Figure 2. A double S-shaped curve can be recognized, with inflection points occurring at $n(\mathrm{NH_3}) \cdot n(\mathrm{Np})_{\mathrm{initial}}^{-1}$ = 3.74 and 5.51 (pH 3.6 and pH 6.5,

respectively). A selection of absorption spectra measured from the sample aliquots with corresponding identifiers S0 to S39 is presented in Figure 3 (a) and (b). From the start of the experiment (spectrum S0, pH 1.6) until just before the first inflection point (spectrum S18, pH 2.7) the spectra remain almost unchanged, and the rate of pH increase appears to be mostly limited by the neutralization reaction between free NO_3^- and NH_3. A small shift in the fine structure between 400 − 500 nm can be distinguished, and a very limited decrease in absorbance at the 1223 nm absorption band is observed. These changes can relate to a variation in the coordination environment around the NpO_2^{2+} ions, where bidentate-coordinating nitrate ions are being replace by hydrated water molecules.[33]. Subtle spectral change may also be introduced by a shift in the equilibrium between soluble polymeric hydrolysis products of Np(VI).[46]

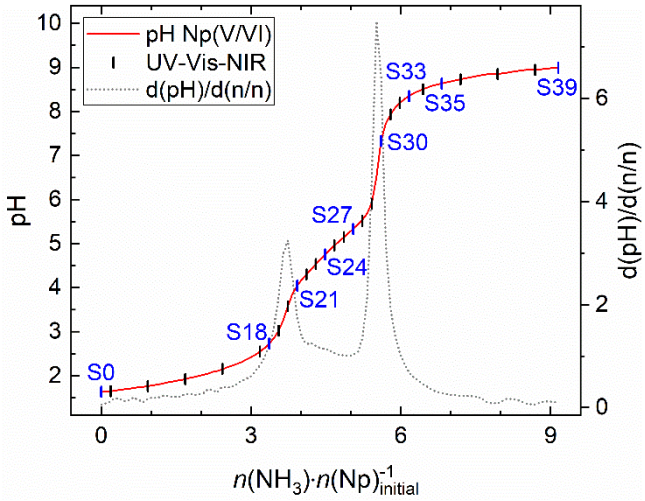

Figure 2. pH evolution in the Np(V)/Np(VI) solution during titration with NH_3 aq. solution at room temperature. Vertical lines denote points at which samples were taken for UV-Vis-NIR analysis. The corresponding identifiers are ascending from S0 to S39, a selection is printed and highlighted in blue color for clarity towards the reader.

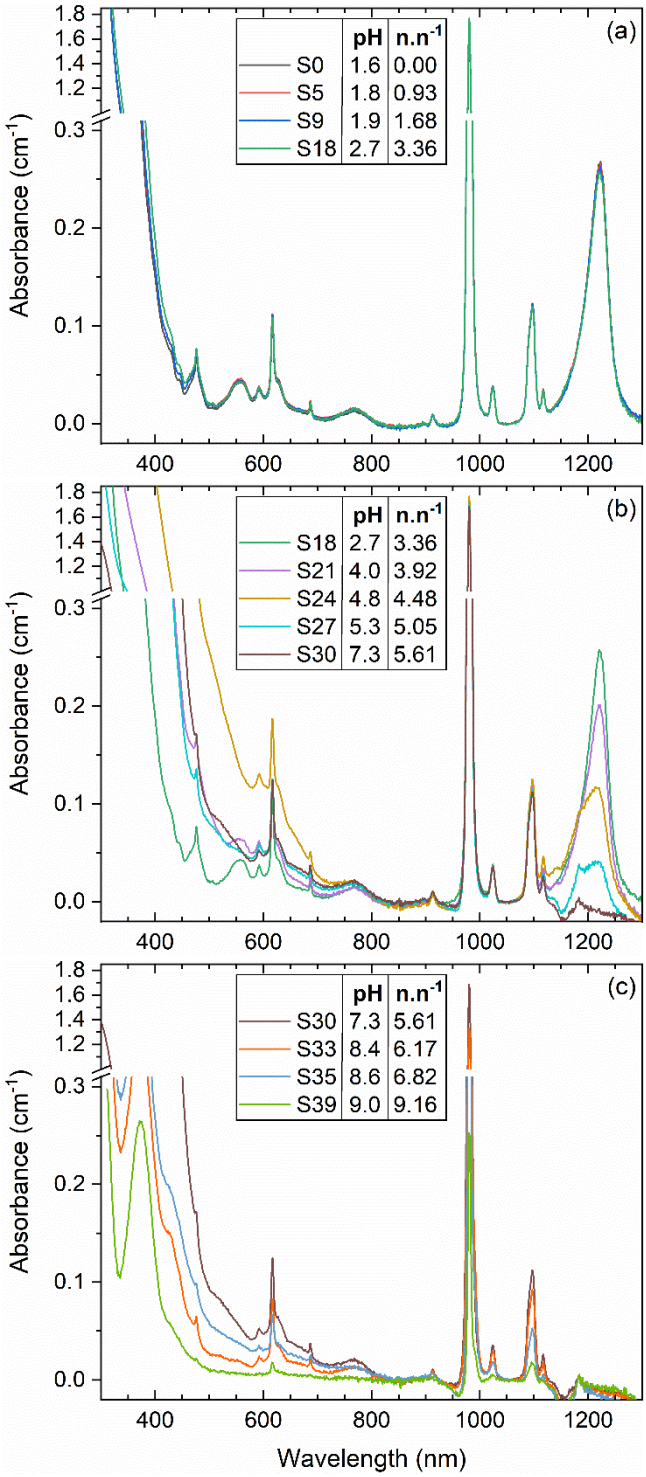

Figure 3. Selection of UV-Vis-NIR absorption spectra from the sample aliquots taken during the hydrolysis experiment. The corresponding pH value and molar ratio of NH_3 (aq.) to initial neptunium ($n\ n^{-1}$) are presented in the legend. (a) Spectra S0 to S18 (pH 1.6 to 2.7) do not show any notable changes in the Np absorption bands; they correspond to the onset of the experiment during which free NO_3^- was neutralized with NH_3. (b) Spectra S18 to S30 (pH 2.7 to 7.3) show a systematic decrease in the Np(VI) absorption band around 1223 nm. (c) Spectra S30 to S39 (pH 7.3 to 9.0) show a systematic decrease in the remaining Np(V) absorption bands.

At increased pH levels a systematic decrease in the 1223 nm band, which is associated to Np(VI), occurs (spectra S21, pH 4.0; S24, pH 4.8; S27, pH 5.3), and near the second inflection point (spectrum S30, pH 7.3) this band is reduced to the baseline level. Conversely, in the pH interval from 2.7 to 7.3, the absorption bands associated to Np(V) remain rather unchanged, which indicates that the corresponding hydrolysis reaction involves predominantly Np(VI) ions.

At pH values above 7.3, *i.e.* after the second inflection point, a notable decrease in absorbance of the remaining absorption bands, which are associated to Np(V), occurs (spectrum S35, pH 8.6, in Figure 3 (c)). The most intense bands at 980 and 1098 nm are still observed after reaching a pH level of 9.0 (spectrum S39) but the corresponding Np(V) concentration has decreased to approximately 6% of the initial, total Np concentration. Cleary, the hydrolysis and precipitation of Np(V) requires a much more elevated pH range as compared to Np(VI).

A visual color change of the solution and the eventual formation of a red/brown colored precipitate was observed during the experiment between pH 3.9 and 5.0 (see Figure S2 in the ESI). This coincides with the significantly elevated baseline level seen in the corresponding absorption spectra (S21 to S24), specifically in the UV to visible region. Likely, under the experimental conditions small colloids were formed (presumably $NpO_3 \cdot H_2O$, based on the color of the precipitate)[48] which could not be effectively separated from the supernatant solution in the sampled aliquots.

3.3.Preparation and hydrolysis of Np(V)

A second hydrolysis experiment was intended on a single-valence Np(V) solution prepared from the Np stock solution. In order to obtain the starting solution, an aliquot of the stock solution was first transferred into a round-bottom flask and diluted with Milli-Q water to obtain c(Np) = 0.013 mol/L. Secondly, incremental amounts of NH_3 aq. solution were added to neutralize most of the free NO_3^- remaining from the stock solution. Based on the position of the first inflection point found during the hydrolysis test described in §3.2, NH_3 aq. solution was added until $n(\mathrm{NH_3}) \cdot n(\mathrm{Np})^{-1}_{\mathrm{initial}}$ = 3.58 was reached (pH 3.1).

Reduction of the Np(VI) present in the stock solution into Np(V) was subsequently achieved by adding a small amount (125 µL) of a freshly-prepared $NaNO_2$ aq. solution (0.5 mol/L) to the flask. Upon addition of $NaNO_2$, the color of the Np solution immediately turned from a greenish tint to light blue, see Figure S3 in the ESI. Due to addition of the aforementioned

aqueous reactants the Np concentration was diluted from the initial value of 0.013 mol/L to 0.01 mol/L, as was targeted for the subsequent hydrolysis experiment. A comparison of absorption spectra acquired during these preparation steps is presented in Figure 4.

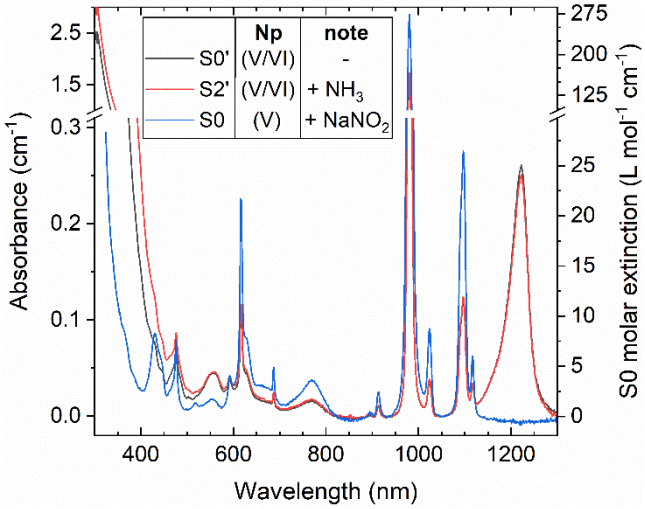

Figure 4. Selection of UV-Vis-NIR absorption spectra taken during preparation of the Np(V) solution. Spectra S0' and S2' show absorption bands corresponding to Np(V) and Np(VI), similar as in the Np stock solution. The neutralization of free NO_3^- by NH_3 does not lead to notable changes in spectrum S2'. Spectrum S0 was measured just after addition of $NaNO_2$ and is representative of single valence Np(V). The molar extinction corresponding to spectrum S0 is presented on the right-hand side abscissa.

Spectra S0' and S2' show no significant changes in the Np absorption bands, apart from the small shifts between 400 − 500 nm and at the broad band centered around 1223 nm which were similarly observed in the Np(V)/Np(VI) hydrolysis experiment reported in section §3.2. The addition of $NaNO_2$ induced a significant change in absorption spectrum S0: The absorption bands associated to Np(VI), e.g. around 1223 nm, have disappeared completely with a corresponding increase in the absorption bands associated to Np(V). Also no absorption bands associated to any of the lower valence states of Np were observed,[45,54] thus confirming the formation of a single-valence Np(V) solution.

Hydrolysis in the Np(V) solution was investigated in the same manner as reported for the mixed Np(V)/Np(VI) solution in §3.2, i.e. by the controlled addition of NH_3 aq. solution. The pH evolution as function of added NH_3 is presented in Figure 5. The initial section of the diagram up to $n(\mathrm{NH_3}) \cdot n(\mathrm{Np})^{-1}_{\mathrm{initial}} = 3.58$ corresponds to the Np(V) preparation steps described above, i.e. the initial neutralization of free NO_3^- by NH_3 in the starting solution between pH 1.4 to 3.2, and the subsequent addition of $NaNO_2$ which caused a discrete drop in

pH to 2.2. The onset of the Np(V) hydrolysis experiment is marked by a rapid pH increase, with the inflection point occurring at $n(\mathrm{NH_3}) \cdot n(\mathrm{Np})^{-1}_{\mathrm{initial}}$ = 4.43 (pH 5.5). A selection of absorption spectra measured from the sample aliquots with corresponding identifiers S0 to S24 is presented in Figure 6 (a) and (b).

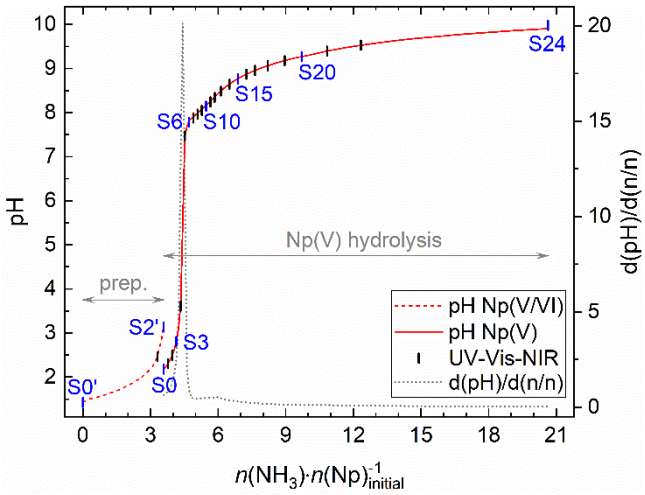

Figure 5. (dashed red line) pH evolution during preparation of the Np(V) solution. Vertical lines denote points at which samples were taken for UV-Vis-NIR analysis. The corresponding identifiers are ascending from S0' to S2' and from S0 to S24; a selection is printed and highlighted in blue color for clarity towards the reader. (solid red line) pH evolution in the Np(V) solution during titration with NH_3 aq. solution at room temperature.

At pH levels of 7.8 and above solid precipitates were distinguished in the sample aliquot (see Figure S4 in the ESI) and a notable decrease in overall absorbance occurred (spectrum S6, pH 7.8). At higher pH levels, hydrolysis and precipitation continued systematically and the absorption bands dropped to background levels when reaching a pH of 9.3 (spectrum S20), except for the most intense absorption band at 980 nm, associated to the free NpO_2^+ ion.[41] Finally, at a pH value of 10, the 980 nm band also disappeared (spectrum S24), indicating that all Np had precipitated from the solution. In the near-infrared spectral region, some negative absorption values were measured, likely associated to a mismatch between the baseline medium (Milli-Q water) and increased concentrations of NH_3 (aq.) and by-products such as ammonium nitrate in the sample solution. At the end of the experiment the round-bottom flask contained an off-white colored precipitate, indicative of the hydroxide NpO_2OH.

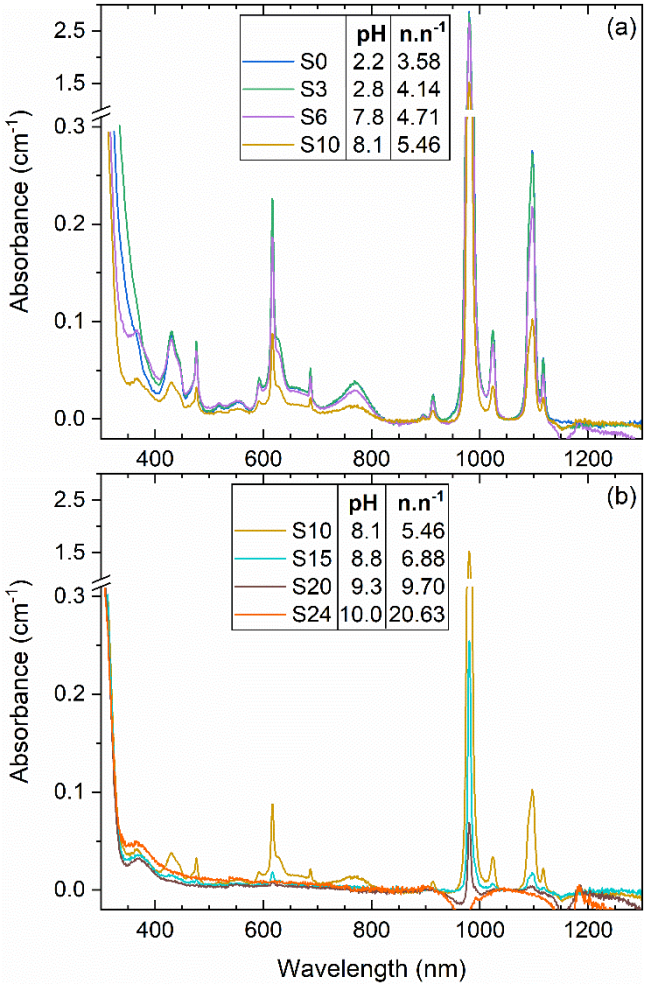

Figure 6. Selection of UV-Vis-NIR absorption spectra from the sample aliquots taken during the hydrolysis experiment. The corresponding pH value and molar ratio of NH_3 (aq.) to initial neptunium ($n\ n^{-1}$) are presented in the legend. (a) Spectra S0 to S10 (pH 2.2 to 8.1) show a systematic decrease in the Np(V) absorption bands. (b) Spectra S10 to S24 show that pH levels up to 10.0 were required to reduce the intense band at 980 nm to background level.

3.1.Hydrolysis of U(VI)

The pH evolution in the U(VI) solution as function of added NH_3 aq. solution (expressed as the molar ratio of NH_3 (aq.) to initial uranium during the experiment, $n(\mathrm{NH_3}) \cdot n(\mathrm{U})^{-1}_{\mathrm{initial}}$) is presented in Figure 7. Again, a double S-shaped curve can be recognized, with inflection points occurring at $n(\mathrm{NH_3}) \cdot n(\mathrm{U})^{-1}_{\mathrm{initial}}$ = 1.85 and 2.63 (pH 5.1 and pH 6.8, respectively). A selection of absorption spectra measured from the sample aliquots with corresponding identifiers S0 to S23 is presented in Figure 8 (a) and (b). The spectrum of the initial solution is characterized by a broad but relatively weak absorption band between 350 and 500 nm,

having a specific fine structure which results from symmetric stretching vibration and coupled electronic transitions of the uranyl (UO_2^{2+}) ion.[57,58]

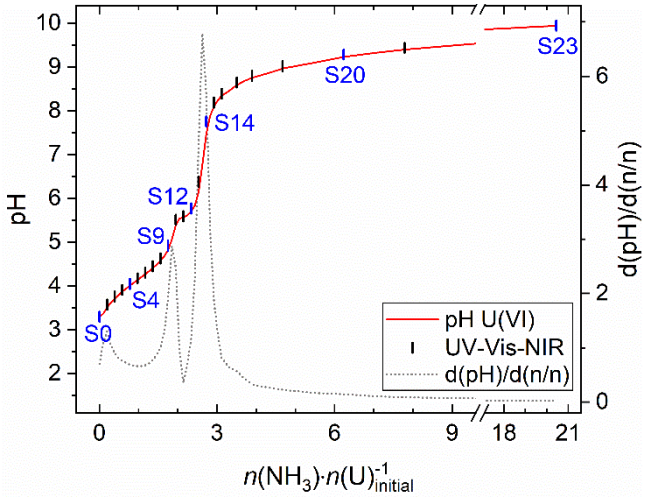

Figure 7. pH evolution in the U(VI) solution during titration with NH_3 aq. solution at room temperature. Vertical lines denote points at which samples were taken for UV-Vis-NIR analysis. A selection of identifiers is printed and highlighted in blue color for clarity towards the reader.

At the onset of the titration and until just before the first inflection point (spectrum S9, pH 4.9) a gradual increase in absorbance and notable shift in the fine structure occurs. Changes in the nitrate and acid concentrations are known to affect the ratio between the intensity of the local maxima between 400 nm and 430 nm.[59] More importantly, however, are the hydrolyzed uranyl species of the general form $(UO_2)_x(OH)_y^{(2x-y)+}$, which are expected to be formed under the applied experimental conditions.[60] Each spectrum is actually a convolution of the absorption bands associated to UO_2^{2+}, $(UO_2)_2(OH)_2^{2+}$ and $(UO_2)_3(OH)_5^{+}$ in different ratios.[60,61] Additionally, due to uptake of atmospheric CO_2 in the solution, solid UO_2CO_3 or aqueous uranyl carbonate complexes could be formed as well.[58,62] We note that a quantified distribution of the oligomeric hydrolysis species can be obtained by performing factor analysis on the spectra, as reported extensively in the works of Meinrath,[58,61] but this is not the focus of the current study. Based on the initial concentration, and taking into account the dilution imposed by the titration, the molar extinction corresponding to each spectrum was derived and plotted on the right-hand side abscissa of Figure 8 (a).

At pH levels above 4.9 a fast, systematic decrease in the absorbance occurs, and a corresponding increase in turbidity of the solution was observed (see Figure S5 in the ESI), which indicates an insoluble hydrolysis species was formed. One or more solid phases from

the system NH_3 – UO_3 – H_2O are typically formed under the applied experimental conditions, generically referred to as ammonium diuranate.[63,64] Background absorption levels in the visible region (above 400 nm) were reached between pH 6.4 (S13) and pH 7.8 (S14).

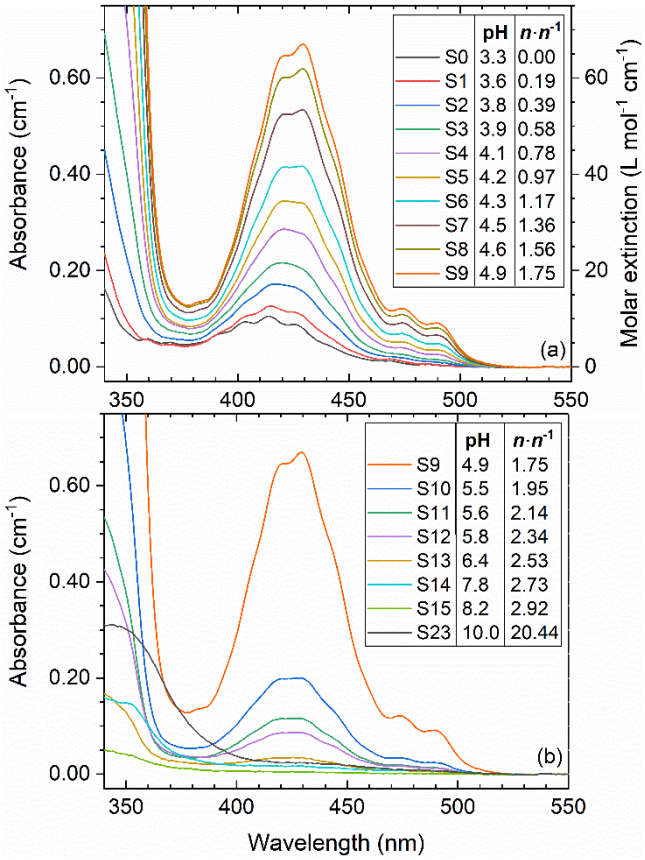

Figure 8. Selection of UV/VIS absorption spectra measured from the sample aliquots taken during the U(VI) hydrolysis experiment. The corresponding pH value and molar ratio of NH_3 (aq.) to initial uranium ($n\ n^{-1}$) are presented in the legend. (a) Spectra S0 to S9 (pH 3.3 to 4.9) show a strong increase in absorbance and shift in the fine structure of the spectral band between 400 and 450 nm, associated to formation of soluble hydrolysis products. (b) Spectra S10 to S23 (pH 5.5 to 10.0) show a rapid decrease in absorbance of the U(VI) bands as the pH increases.

4. Discussion

To evaluate the suitability of each Np species for sol-gel conversion processes either as the matrix element, or as a dopant together with uranium, a comparison of the hydrolysis behavior and precipitation regimes is necessary. The hydrolysis experiments on the single-valence Np(V) and U(VI) solutions, combined with results on the mixed Np(V)/Np(VI) solution, allow to clearly differentiate the behavior of the individual species NpO_2^+, NpO_2^{2+} and UO_2^{2+} during titration with aqueous ammonia. To enhance the data assessment the concentration of neptunium and uranium species, and their evolution during hydrolysis were deduced from the UV-Vis-NIR absorbance of well-differentiated absorption bands and the corresponding reported molar extinctions. For U(VI) the absorbance and molar extinction at 429.5 nm was used, i.e. the wavelength at which the local maximum of the broad absorption band between 370 and 500 nm occurred in sample S9. To take into account the dependency between molar extinction and pH,[58] the corresponding values were taken from Figure 8 (a) up to pH 4.9. At higher pH values the molar extinction determined at pH 4.9 (66.7 L mol^{-1} cm^{-1}) was assumed to remain constant over the remaining pH interval.

For Np(V) and Np(VI) the absorbance and corresponding molar extinctions at 1097 nm and at 1223 nm, respectively, were used (see also section §3.1). While changes can be induced to these molar extinction values by variations in nitric acid concentration (e.g. between 0.50 and 4.00 mol L^{-1}),[54] this dependency is unclear at the lower range of nitrate concentration and at the elevated pH values reached in this work. Therefore, the molar extinction values were assumed to remain constant over the entire pH interval. The results reported in Figure 9 illustrate the differences and similarities between the metal ions in nitric acid environment during hydrolysis by addition of NH_3, and their implications will now be discussed in more detail.

In the Np(V)/Np(VI) mixed solution, an increase in the lower pH range from pH 1.6 to pH 3.5, corresponding to the interval up to the first inflection point, did not induce significant changes in the absorption spectrum. Only a subtle decrease in the maximum of the broad band centered around 1223 nm (associated to NpO_2^{2+}) was observed, which results in a decreasing trend in the Np(VI) concentration from the onset of the curve presented in Figure 9 (a). However, realizing there could be a dependency between the 1223 nm molar extinction and the nitrate concentration,[54] the Np(VI) concentration actually may have remained constant in the low pH region. Similar behavior, although much more pronounced, was observed during the U(VI) hydrolysis where the ratio of oligomeric hydrolysis species is affected by pH, but

the total U(VI) concentration in solution remains constant until precipitation occurs. At pH values above 3.5 a more drastic decrease of the 1223 nm absorption band took place, congruent also with a color change of the solution and formation of a red/brown colored precipitate (see Figure S2 in the ESI). Kato *et al.* reported on the characterization of such a dark reddish-brown precipitate as $NpO_3 \cdot H_2O$, while performing solubility studies on Np(VI).[48] However, other solid phases such as $NpO_3 \cdot 2H_2O$ and $NpO_2(OH)_2$ have been reported to form as well.[47] No NpO_2^{2+} remained in solution at pH values above pH 5.9.

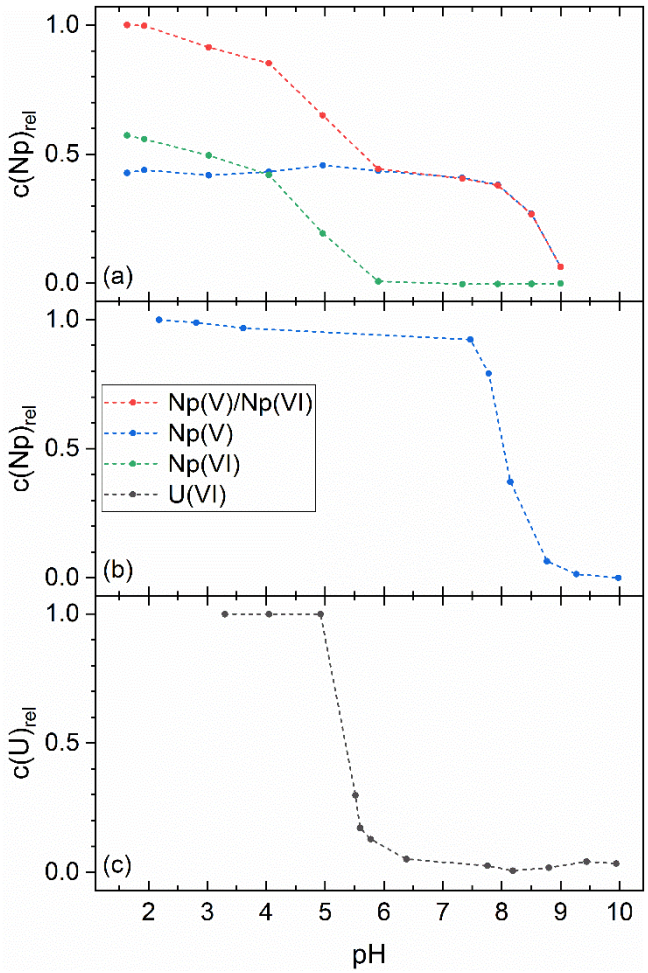

Figure 9. Evolution of the individual Np(V), Np(VI) and U(VI) cation concentrations and of the combined Np(V)/Np(VI) concentration as function of pH during the hydrolysis experiments. Concentrations are derived from the UV-Vis-NIR absorbance of a well-differentiated absorption band and the reported molar extinctions for these bands (see text for details), and expressed relative to the initial actinide concentration. (a) Results from the hydrolysis experiment on the Np(V)/Np(VI) mixed solution, (b) on the Np(V) solution, (c) on the U(VI) solution.

The hydrolysis behavior of Np(V) appears more straight-forward. In the Np(V)/Np(VI) mixed solution the concentration of Np(V) as determined from the 1097 nm absorption band was not affected up to a pH value of 7.5. In the single-valence Np(V) solution a very minor decrease in the maximum of the 1097 nm absorption band was observed, resulting in a slightly decreasing initial trend in the Np(V) concentration presented in Figure 9 (b). Considering the presence of Na^+ ions from using $NaNO_2$ in the solution preparation steps, the apparent drop in solubility can be correlated to formation of sodium salts of anionic neptunium species,[65] or even incorporation of Na^+ in NpO_2OH.[66] Nevertheless, NpO_2^+ remained the predominant species in solution until the pH exceeded 7.5, after which a systematic decrease in absorbance and corresponding strong decrease in concentration occurred, associated to hydrolysis into the off-white colored, insoluble hydroxide NpO_2OH (see Figure S4 in the ESI).[40] At a pH of 9.0, a small fraction of NpO_2^+ (3 % of the total amount) remained in solution, whereas at a pH of 10.0 no remaining amounts were detected.

The pH regime for Np(V) hydrolysis is similar to that reported by Rao *et al*., using $(CH_3)_4NCl$ as the background electrolyte in HCl solution.[41] In contrast, Neck *et al*. reported that no significant Np(V) hydrolysis occurred in carbonate-free perchlorate solutions at pH below 10.[40] This remarkable difference in the hydrolytic properties of Np(V) was debated in literature,[42,44] and following critical reviews it was assigned to the effect of carbonate complexation due to infiltration of CO_2 during the experiments by Rao *et al*.[43,47] In the present experiments no protective environment was applied, and hence, interaction with CO_2 cannot be ruled out. The extent of carbonate complexation can be assessed from the spectrophotometric data, as it is associated to a distinct absorption band at 991 nm, or as a shoulder on the intense 980 nm band, depending on exposure time.[29,40,43] Only a small shoulder could be observed at 991 nm in our experiments, compared to the appearance of much stronger absorbance effects reported in literature (see Figure S6 in the ESI).[40,41,43] Nevertheless, to perform a detailed assessment of the hydrolytic properties of Np in nitrate medium, dedicated experiments under controlled conditions of carbonate concentration are still required.

The hydrolysis of U(VI) in the pH interval 3.3 to 4.9 was characterized by significant shifts in the spectral bands, associated to changes in the equilibrium between UO_2^{2+} ions and the oligomeric species $(UO_2)_2(OH)_2^{2+}$ and $(UO_2)_3(OH)_5^+$. Based on the extensive literature on this topic,[58,59] the total U(VI) concentration was assumed constant, allowing to derive the molar extinction corresponding to each (convoluted) spectrum. Upon exceeding pH 4.9 an

immediate decrease in absorbance was observed, congruent with an increase in solution turbidity and precipitation of an ammonium diuranate precipitate (see Figure S5 in the ESI). Above pH 6.4 the U(VI) concentration reached background levels, see Figure 9 (c).

There is a clear and significant discrepancy between the pH interval for hydrolysis and precipitation of Np(V) and of Np(VI) or U(VI) solutions. These results show clearly that any sol-gel process aimed at producing homogeneously gelled kernels should not consider a mixture of Np(V)/Np(VI) or Np(V)/U(VI) as feed broth. For pure Np kernels, either Np(V) or Np(VI) will be possible. For mixed U-Np systems, Np(VI)/U(VI) feed broths are preferred since the hydrolysis behavior of Np(VI) and U(VI) match well to each other, with precipitation occurring in a largely overlapping pH interval between 4.0 and 6.4.

The inherent differences between the sol-gel technologies internal and external gelation further impose certain restrictions. As was mentioned in the introduction, external gelation uses gaseous and/or aqueous NH_3 to achieve the necessary pH increase of the feed broth to hydrolyze and precipitate. Typically, the aqueous NH_3 solution concentration is around 4 mol L^{-1},[67] which corresponds to a pH value well above pH 11. This is compatible to hydrolyze and precipitate all species considered in this work, both at the presently used ionic strength (c(Np) = c(U) = 0.01 mol L^{-1}) and at conventional process conditions relying on a cation concentration of the order 1 mol L^{-1} in the feed broth, which will shift the pH profile more to the left. For external gelation processes, no further restrictions on the feed broth than those mentioned above, would be needed.

Internal gelation, on the other hand, relies on the thermal decomposition of gelation agents (hexamethylenetetramine and urea), resulting in a fast, *in-situ* release of NH_3. Collins *et al*. reported a comprehensive study on the chemistry involved with internal gelation of uranium feed broths, and demonstrated the pH evolution in the broth to vary between pH 3.7 and pH 6.0 at gelation temperatures between 0 °C and 92 °C, while also depending on other process conditions such as the concentration of uranium and the gelation agents.[68] At the elevated temperature applied during internal gelation the hydrolysis of Np(V) will increase, but similarly, this is the case for U(VI). Therefore, the typical process conditions used for processing uranium feed broths will not be directly transferrable to achieve complete precipitation of Np(V). A change in the conditions such as using different amounts of gelation agents is known to affect the stability of a feed broth and may induce premature gelation.[68,69] Furthermore, urea is a known scavenger for HNO_2 which may induce reoxidation of Np(V) to Np(VI).[70] Therefore, conventional internal gelation process conditions seem incompatible

with a feed broth containing Np(V), and further research efforts would be required to find out if suitable conditions can be reached. However, a successful application can be expected on a Np(VI) or mixed Np(VI)/U(VI) feed broth due to their similar response.

5. Conclusion

The speciation and hydrolysis of oxygenated neptunium (NpO_2^+ and NpO_2^{2+}) and uranyl ions (UO_2^{2+}) in nitric acid have been investigated during titration with aqueous NH_3 solution. UV-Vis-NIR spectrophotometry was used to measure changes in the absorption spectra of the prepared solutions, following a pH evolution from acidic (pH 1.5) to alkaline (pH 10) conditions at room temperature. The combined results allowed to evaluate the suitability of Np(V) or Np(VI) in sol-gel conversion processes either as the matrix element, or as a dopant together with uranium.

In the pH interval between pH 1.6 to pH 7.5 Np(V) remains stable and largely unaffected in solution. At pH values above 7.5 hydrolysis into the insoluble hydroxide NpO_2OH takes place. Under the applied experimental conditions a pH increase up to pH 10.0 is required to hydrolyze all NpO_2^+ in solution. Np(VI) is affected immediately upon increase of the pH above 1.6, likely related to changes in the coordination environment of NpO_2^{2+} ions or hydrolyzed species, similar to what is observed for U(VI). Hydrolysis into an insoluble hydroxide (e.g. $NpO_3{\cdot}H_2O$) occurs in the pH interval 4.0 – 5.9. U(VI) hydrolyzes and precipitates into ammonium diuranate species mainly between pH values 4.9 – 6.4, which overlaps largely with the corresponding pH interval of Np(VI).

External gelation conditions, making use of concentrated NH_3 aqueous solution as gelation medium, are compatible to fully hydrolyze and precipitate Np(V) or Np(VI) from nitric acid solutions. However, no homogeneous precipitation will occur when a mixture of Np(V)/Np(VI) solution is used in the feed broth, owing to the significantly different hydrolysis regimes with pH. Similarly, a feed broth consisting of Np(V) and U(VI) will not be appropriate for fabricating mixed-oxide microspheres. The alternative solution is to use Np(VI) in conjunction with U(VI) due to their very similar hydrolysis behavior. Internal gelation process conditions, on the other hand, seem incompatible with feed broths containing Np(V) because the required pH increase may not be reached. A successful application can nevertheless be expected on a Np(VI) or mixed Np(VI)/U(VI) feed broth.

Acknowledgements

The authors wish to thank K. Vanaken, P. Dries and E. Kox for laboratory assistance, and the Radiochemical Analyses group of SCK CEN for performing the ICPMS analyses. The authors also thank A. Moens and G. Sibbens of JRC Geel for providing the NpO_2 feed material that made this work possible. The research presented in this article has received funding from the European Union's Horizon 2020 research and innovation program under grant agreement No. 945077 (project PATRICIA), and was carried out as part of the PULSAR project within the framework of the Euratom Research and Training Programme (grant agreement No. 101061251). Views and opinions expressed are, however, those of the author(s) only and do not necessarily reflect those of the European Union or Euratom. Neither the European Union nor Euratom can be held responsible for them.

Electronic supporting information

Comparison of the U(VI) absorption spectrum to literature. Selection of pictures taken during the hydrolysis experiments, highlighting color changes and precipitation. Near-infrared region of selected UV-Vis-NIR absorption spectra.

References

(1) Shmelev, A. N., Geraskin, N. I., Kulikov, G. G., Kulikov, E. G., Apse, V. A., Glebov, V. B., *The problem of large-scale production of plutonium-238 for autonomous energy sources*, 2020 International Scientific and Practical Conference for Young Specialists, Scientists and Post-Graduates on Nuclear Reactor Physics, ICNRP Volga 2020, 7-11 September 2020 **2020**.

(2) Groh, H. J., Schlea, C. S., *The recovery of Neptunium-237 and Plutonium-238* in *Progress in Nuclear Energy , Series III, Process chemistry - Vol. 4*, Pergamon Press Ltd, Oxford, UK, **1970**.

(3) Salvatores, M., Palmiotti, G., Radioactive waste partitioning and transmutation within advanced fuel cycles: Achievements and challenges. *Progress in Particle and Nuclear Physics* **2011**, *66*, 144-166.

(4) Pillon, S., *3.05 - Actinide-Bearing Fuels and Transmutation Targets* in *Comprehensive Nuclear Materials*, Elsevier, Oxford, **2012**, pp. 109-141.

(5) Groh, H. J., Poe, W. L., Porter, J. A., Development and Performance of Processes and Equipment to Recover Neptunium-237 and Plutonium-238. *Proceedings of the Symposium May 17, 2000: 50 Years of Excellence in Science and Engineering at the Savannah River Site* **2000**, 165-178.

(6) Daily, C. R., McDuffee, J. L., Design Studies for the Optimization of 238Pu Production in NpO2 Targets Irradiated at the High Flux Isotope Reactor. *Nucl. Technol.* **2020**, *206*, 1182-1194.

(7) Urban-Klaehn, J., Miller, D., Gross, B. J., Tyler, C. R., Dwight, C. C., Initial phase of Pu-238 production in Idaho National Laboratory. *Appl. Radiat. Isot.* **2021**, *169*, 109517.

(8) Walker, C. T., Nicolaou, G., Transmutation of neptunium and americium in a fast neutron flux: EPMA results and KORIGEN predictions for the superfact fuels. *J. Nucl. Mater.* **1995**, *218*, 129-138.

(9) Vedder, R. J., *Oak Ridge National Laboratory Preparation of Sintered 237NpO2 Pellets for Irradiation to Produce 238Pu Oxide*, Report Oak Ridge National Lab. (ORNL), Oak Ridge, TN (United States), **2018**.

(10) Rankin, D. T., Burney, G. A., Smith, P. K., Sisson, R. D., Jr., Preparation and characterization of oxalate-based neptunium-237 dioxide powder. *Am. Ceram. Soc., Bull.* **1977**, *56*, 478-483, 486.

(11) Vaidya, V. N., Mukerjee, S. K., Venugopal, V., *Sol gel process for nuclear fuels*, International conference on peaceful uses of atomic energy, New Delhi (India), **2009**.

(12) Schreinemachers, C., Bukaemskiy, A. A., Klinkenberg, M., Neumeier, S., Modolo, G., Bosbach, D., Characterization of uranium neodymium oxide microspheres synthesized by internal gelation. *Progress in Nuclear Energy* **2014**, *72*, 17-21.

(13) Sood, D. D., The role sol- gel process for nuclear fuels-an overview. *J. Sol-Gel Sci. Technol.* **2011**, *59*, 404-416.

(14) Van der Brugghen, F. W., Hermans, M. E. A., Kanij, J. B. W., Noothout, A. J., Van der Plas, T., Slooten, H. S. G., *Sol-gel processes for the preparation of spherical thorium-containing fuel particles.*, Report Keuring van Elektrotechnische Materialen te Arnhem (KEMA), Arnhem, Netherlands, **1968**.

(15) van der Brugghen, F. W., Kanij, J. B. W., Noothout, A. J., Hermans, M. E. A., Votocek, O., *A U(VI)-process for microsphere production*, Symposium on Sol-Gel Processes and Fuel Cycles, Gatlinburg, **1970**.

(16) Collins J, L., Lloyd M, H., Fellows R, L., in *Radiochimica Acta, Vol. 42*, **1987**, p. 121.

(17) Nagarajan, K., Vaidya, V. N., *Sol-Gel Processes for Nuclear Fuel Fabrication* in *Sol-Gel Processing for Conventional and Alternative Energy*, Springer, New York, **2012**.
(18) Ganguly, C., Sol-gel microsphere pelletization: A powder-free advanced process for fabrication of ceramic nuclear fuel pellets. *Bull. Mater. Sci.* **1993**, *16*, 509-522.
(19) Lyon, C. E., The preparation of metal oxide spheres for use in neutron dosimetry. *Nuclear Instruments and Methods in Physics Research Section A: Accelerators, Spectrometers, Detectors and Associated Equipment* **1985**, *236*, 604-608.
(20) Martel, L., Vigier, J. F., Prieur, D., Nourry, S., Guiot, A., Dardenne, K., Boshoven, J., Somers, J., Structural investigation of uranium-neptunium mixed oxides using XRD, XANES, and 17O MAS NMR. *Journal of Physical Chemistry C* **2014**, *118*, 27640-27647.
(21) Vigier, J.-F., Martin, P. M., Martel, L., Prieur, D., Scheinost, A. C., Somers, J., Structural Investigation of $(U_{0.7}Pu_{0.3})O_{2-x}$ Mixed Oxides. *Inorg. Chem.* **2015**, *54*, 5358-5365.
(22) Vigier, J.-F., Freis, D., Pöml, P., Prieur, D., Lajarge, P., Gardeur, S., Guiot, A., Bouëxière, D., Konings, R. J. M., Optimization of Uranium-Doped Americium Oxide Synthesis for Space Application. *Inorg. Chem.* **2018**, *57*, 4317-4327.
(23) Nästren, C., Fernandez-Carretero, A., Somers, J., Synthesis route for the safe production of targets for transmutation of plutonium and minor actinides. *Nucl. Technol.* **2013**, *181*, 331-336.
(24) Suresh Kumar, K., Mathews, T., Nawada, H. P., Bhat, N. P., Oxidation behaviour of uranium in the internally gelated urania–ceria solid solutions – XRD and XPS studies. *J. Nucl. Mater.* **2004**, *324*, 177-182.
(25) Kumar, A., Radhakrishna, J., Kumar, N., Pai, R. V., Dehadrai, J. V., Deb, A. C., Mukerjee, S. K., Studies on preparation of $(U_{0.47},Pu_{0.53})O_2$ microspheres by internal gelation process. *J. Nucl. Mater.* **2013**, *434*, 162-169.
(26) Schreinemachers, C., Influence of redox conditions on the conversion of actinide solutions into microspheres via sol-gel chemistry. *PhD thesis*, KU Leuven **2020**.
(27) Schreinemachers, C., Bollen, O., Leinders, G., Tyrpekl, V., Modolo, G., Verwerft, M., Binnemans, K., Cardinaels, T., Hydrolysis of Uranyl-, Nd-, Ce-Ions and their Mixtures by Thermal Decomposition of Urea. *Eur. J. Inorg. Chem.* **2022**, *2022*, e202100453.
(28) Kessinger, G., Kyser, E., Almond, P., *Literature review: Reduction of Np(V) to Np(IV) - Alternatives to ferrous sulfamate*, Report SRNL-STI-2009-00610; TRN: US1000139, United States, **2009**.
(29) Yoshida, Z., Johnson, S. G., Kimura, T., Krsul, J. R., *Neptunium* in *The Chemistry of the Actinide and Transactinide Elements*, Springer Netherlands, Dordrecht, **2011**, pp. 699-812.
(30) Newton, T. W., Baker, F. B., *Aqueous Oxidation-Reduction Reactions of Uranium, Neptunium, Plutonium, and Americium* in *Lanthanide/Actinide Chemistry, Vol. 71*, American Chemical Society, **1967**, pp. 268-295.
(31) Allard, B., Kipatsi, H., Liljenzin, J. O., Expected species of uranium, neptunium and plutonium in neutral aqueous solutions. *J. Inorg. Nucl. Chem.* **1980**, *42*, 1015-1027.
(32) Gogolev, A. V., Shilov, V. P., Perminov, V. P., Fedoseev, A. M., Photolysis of Neptunium Ions in HCOOH Solutions. *Radiochemistry* **2020**, *62*, 474-479.
(33) Ikeda-Ohno, A., Hennig, C., Rossberg, A., Funke, H., Scheinost, A. C., Bernhard, G., Yaita, T., Electrochemical and Complexation Behavior of Neptunium in Aqueous Perchlorate and Nitrate Solutions. *Inorg. Chem.* **2008**, *47*, 8294-8305.
(34) Runde, W., Neu, M. P., Clark, D. L., Neptunium(V) hydrolysis and carbonate complexation: Experimental and predicted neptunyl solubility in concentrated NaCl using the Pitzer approach. *Geochim. Cosmochim. Acta* **1996**, *60*, 2065-2073.

(35) Swanson, J. L., *Oxidation of Neptunium (V) in nitric acid solution - Laboratory study of rate accelerating materials (RAM)*, Report Battelle Memorial Institute, **1969**.
(36) Siddall, T. H., Dukes, E. K., Kinetics of HNO2 Catalyzed Oxidation of Neptunium(V) by Aqueous Solutions of Nitric Acid1. *J. Am. Chem. Soc.* **1959**, *81*, 790-794.
(37) Marchenko, V. I., Koltunov, V. S., Dvoeglazov, K. N., Kinetics and mechanisms of redox reactions of U, Pu, and Np in tributyl phosphate solutions. *Radiochemistry* **2010**, *52*, 111-126.
(38) Guillaume, B., Moulin, J. P., Maurice, Ch., *Chemical properties of neptunium applied to neptunium management in extraction cycles of PUREX process.*, Symposium on liquid-liquid extraction science, Dounreay (UK), **1984**.
(39) Fellhauer, D., Altmaier, M., Gaona, X., Lützenkirchen, J., Fanghänel, T., Np(V) solubility, speciation and solid phase formation in alkaline CaCl2 solutions. Part II: Thermodynamics and implications for source term estimations of nuclear waste disposal. **2016**, *104*, 381-397.
(40) Neck, V., Kim, J. I., Kanellakopulos, B., Solubility and Hydrolysis Behaviour of Neptunium(V). *Radiochimica Acta* **1992**, *56*, 25-30.
(41) Rao, L., Srinivasan, T. G., Garnov, A. Y., Zanonato, P., Di Bernardo, P., Bismondo, A., Hydrolysis of neptunium(V) at variable temperatures (10–85°C). *Geochim. Cosmochim. Acta* **2004**, *68*, 4821-4830.
(42) Neck, V., Comment on "Hydrolysis of neptunium(V) at variable temperatures (10–85°C)" by L. Rao, T.G. Srinivasan, A.Yu. Garnov, P. Zanonato, P. Di Bernardo, and A. Bismondo. *Geochim. Cosmochim. Acta* **2006**, *70*, 4551-4555.
(43) Spent Fuel Dissolution and Source Term Modelling in Safety Assessment, SKI Report 2007:17, **2007**.
(44) Rao, L., Srinivasan, T. G., Garnov, A. Y., Zanonato, P., Bernardo, P. D., Bismondo, A., Response to the comment by V. Neck on "Hydrolysis of neptunium(V) at variable temperatures (10–85°C)", Geochimica et Cosmochimica Acta 68, 4821–4830. *Geochim. Cosmochim. Acta* **2006**, *70*, 4556-4562.
(45) Friedman, H. A., Toth, L. M., Absorption spectra of Np(III), (IV), (V) and (VI) in nitric acid solution. *J. Inorg. Nucl. Chem.* **1980**, *42*, 1347-1349.
(46) Cassol, A., Magon, L., Tomat, G., Portanova, R., Soluble intermediates in the hydrolysis of neptunium(VI) and comparison with other actinides(VI). *Inorg. Chem.* **1972**, *11*, 515-519.
(47) Brown, P. L., Ekberg, C., *Actinide Metals* in *Hydrolysis of Metal Ions*, **2016**, pp. 325-432.
(48) Kato, Y., Kimura, T., Yoshida, Z., Nitani, N., Solid-Liquid Phase Equilibria of Np(VI) and of U(VI) under Controlled CO2 Partial Pressures. *Radiochimica Acta* **1996**, *74*, 21-26.
(49) Richter, K., Sari, C., Phase relationships in the neptunium-oxygen system. *J. Nucl. Mater.* **1987**, *148*, 266-271.
(50) Menges, F., *"Spectragryph - optical spectroscopy software", Version 1.2.15* http://www.effemm2.de/spectragryph/, **2021**, accessed on:
(51) Magnusson, L. B., Huizenga, J. R., Stabilities of +4 and +5 Oxidation States of the Actinide Elements—the Np(IV)-Np(V) Couple1 in Perchloric Acid Solution. *J. Am. Chem. Soc.* **1953**, *75*, 2242-2246.
(52) Hagan, P. G., Cleveland, J. M., The absorption spectra of neptunium ions in perchloric acid solution. *J. Inorg. Nucl. Chem.* **1966**, *28*, 2905-2909.
(53) Azam, S., Reshak, A. H., Theoretical calculations for MUO3 (M = Na; K; Rb): DFT + U study. *J. Organomet. Chem.* **2014**, *766*, 22-33.

(54) Chatterjee, S., Bryan, S. A., Casella, A. J., Peterson, J. M., Levitskaia, T. G., Mechanisms of neptunium redox reactions in nitric acid solutions. *Inorg. Chem. Frontiers* **2017**, *4*, 581-594.
(55) Mitchell, M., Muftakhidinov, B., Winchen, T., *"Engauge Digitizer Software". Webpage: http://markummitchell.github.io/engauge-digitizer*, accessed on: February 15
(56) Dukes, E. K., Shuler, W. E., *Spectrophotometric Determination of Np(IV) and Np(V) in HNO3 solutions. DP-543*, Report DP-543, **1960**.
(57) Rabinowitch, E., *Absorption spectra of uranyl compounds in solution*, Report ANL-5173, Argonne National Laboratory, Lemont, Illinois, **1953**.
(58) Meinrath, G., Aquatic Chemistry of Uranium A Review Focusing on Aspects of Environmental Chemistry. *Freiberg On-line Geoscience Volume 1* **1998**.
(59) Smith, N. A., Cerefice, G. S., Czerwinski, K. R., Fluorescence and absorbance spectroscopy of the uranyl ion in nitric acid for process monitoring applications. *J. Radioanal. Nucl. Chem.* **2013**, *295*, 1553-1560.
(60) Meinrath, G., Uranium(VI) speciation by spectroscopy. *J. Radioanal. Nucl. Chem.* **1997**, *224*, 119-126.
(61) Meinrath, G., Chemometric analysis: Uranium(VI) hydrolysis by UV-Vis spectroscopy. *J. Alloys Compd.* **1998**, *275-277*, 777-781.
(62) Kramer-Schnabel, U., Bischoff, H., Xi, R. H., Marx, G., Solubility Products and Complex Formation Equilibria in the Systems Uranyl Hydroxide and Uranyl Carbonate at 25°C and I = 0.1 M. **1992**, *56*, 183-188.
(63) Cordfunke, E. H. P., On the uranates of ammonium—I: The ternary system NH3.UO3.H2O. *J. Inorg. Nucl. Chem.* **1962**, *24*, 303-307.
(64) Schreinemachers, C., Leinders, G., Modolo, G., Verwerft, M., Binnemans, K., Cardinaels, T., The conversion of ammonium uranate prepared via sol-gel synthesis into uranium oxides. *Nucl. Eng. Tech.* **2020**, *52*, 1013-1021.
(65) Sullivan, J. C., Choppin, G. R., Rao, L. F., Calorimetric Studies of NpO+2 Hydrolysis. **1991**, *54*, 17-20.
(66) Petrov, V. G., Fellhauer, D., Gaona, X., Dardenne, K., Rothe, J., Kalmykov, S. N., Altmaier, M., Solubility and hydrolysis of Np(V) in dilute to concentrated alkaline NaCl solutions: formation of Na–Np(V)–OH solid phases at 22 °C. **2017**, *105*, 1-20.
(67) Pouchon, M. A., *14 - Gelation and other innovative conversion processes for aqueous-based reprocessing and recycling of spent nuclear fuels* in *Reprocessing and Recycling of Spent Nuclear Fuel*, Woodhead Publishing, Oxford, **2015**, pp. 353-369.
(68) Collins, J. L., Lloyd, M. H., Fellows, R. L., The basic chemistry involved in the Internal-Gelation Method of precipitating uranium as determined by pH measurements. *Radiochimica Acta* **1987**, *42*, 121-134.
(69) Vaidya, V. N., Mukherjee, S. K., Joshi, J. K., Kamat, R. V., Sood, D. D., A study of chemical parameters of the internal gelation based sol-gel process for uranium dioxide. *J. Nucl. Mater.* **1987**, *148*, 324-331.
(70) Fitzpatrick, J., Meyer, T. A., O'Neill, M. E., Williams, D. L. H., Comparison of the reactivity of nine nitrous acid scavengers. *J. Chem. Soc., Perkin Trans. 2* **1984**, 927-932.

TOC graphic

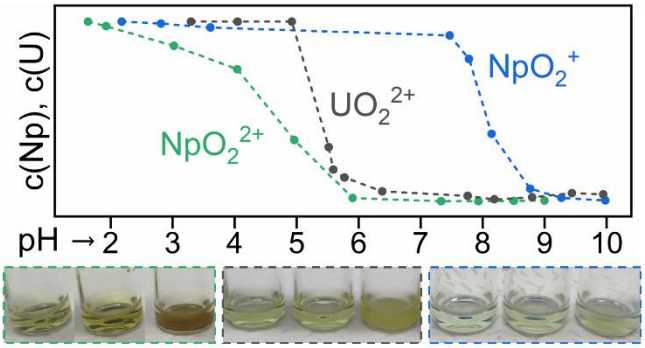

Synopsis

The speciation and associated precipitation regimes of neptunyl (NpO_2^+ and NpO_2^{2+}) and uranyl ions (UO_2^{2+}) in nitric acid during titration with aqueous NH_3 solution were investigated. Np(VI) and U(VI) hydrolyze and precipitate in a largely overlapping pH interval between 4.0 – 6.5, whereas Np(V) requires much more elevated values between pH 7.5 – 10.0. The results offer boundary conditions to the use of sol-gel conversion processes to prepare target materials containing these actinide elements.